Toward the accurate neutrino energy reconstruction in CCQE scattering off nuclear targets

Artur M. Ankowski
Okayama University

based on
A. M. A, Omar Benhar, and Makoto Sakuda, arXiv:1404.5687

NuInt14
Surrey, UK, 19-24 May 2014

Outline

1. Impulse approximation approach and final state interactions
2. Comparisons to electron-carbon scattering data
3. Neutrino energy reconstruction
4. Summary

Impulse approximation approach and final state interactions

Impulse approximation (IA)

Assumption: the dominant process of lepton-nucleus interaction is scattering off a single nucleon, the remaining nucleons act as a spectator system.

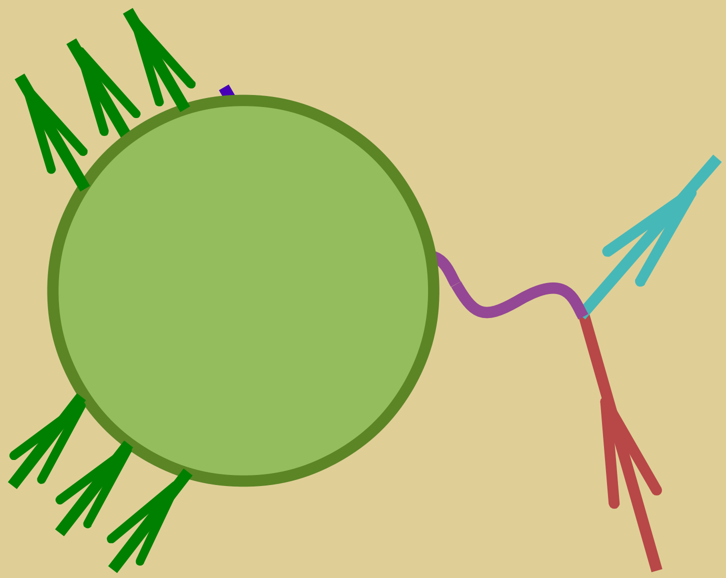

Impulse approximation (IA)

Assumption: the dominant process of lepton-nucleus interaction is scattering off a single nucleon, the remaining nucleons act as a spectator system.

It is valid when the momentum transfer $|\mathbf{q}|$ is high enough, as the probe's spatial resolution is $\sim 1/|\mathbf{q}|$.

Results at
$140 \lesssim |\mathbf{q}| \lesssim 450$ MeV
$0.02 \lesssim Q^2 \lesssim 0.20$ GeV^2

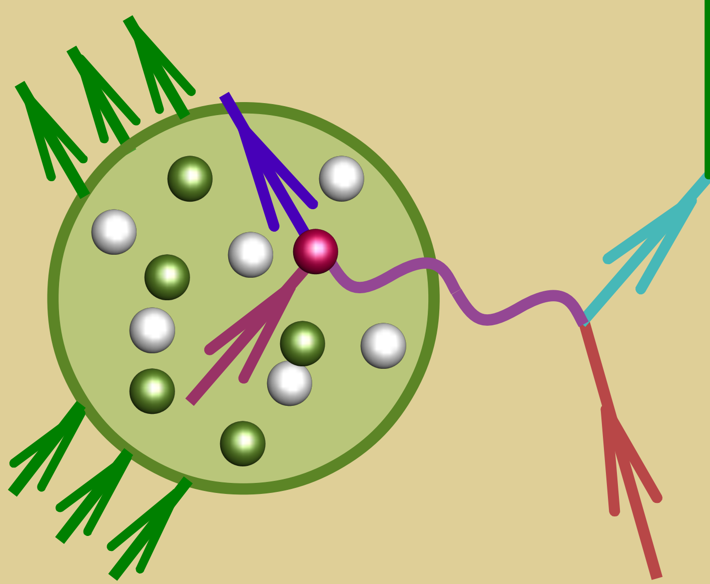

Impulse approximation (IA)

The simplest implementation of the IA assumes that the struck nucleon is on the mass shell ($E_p = \sqrt{M^2 + p^2}$), neglecting its interactions with the spectator system.

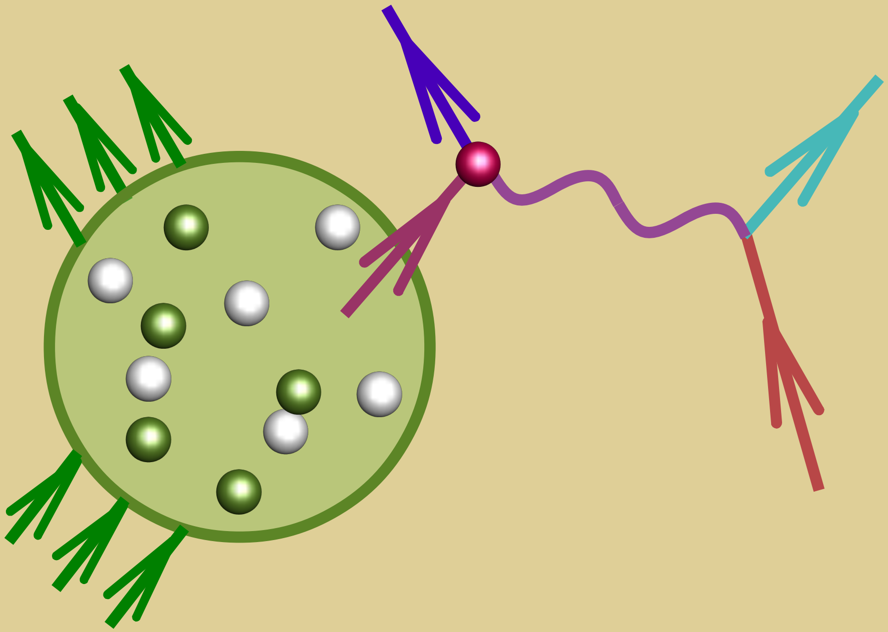

Picture idea from Alberico *et al.*, NPA 623, 471 (1997)

Impulse approximation (IA)

Then, the cross section is

Elementary cross section

$$\frac{d\sigma^{\mathrm{IA}}_{\ell N}}{d\omega d\Omega} = \int d^3p\, dE\, P^N_{\mathrm{hole}}(\mathbf{p}, E)\, \frac{M}{E_{\mathbf{p}}} \frac{d\sigma^{\mathrm{elem}}_{\ell N}}{d\omega d\Omega}\, P^N_{\mathrm{part}}(\mathbf{p}', \mathcal{T}')$$

Hole spectral function

Particle spectral function ~δ(...)

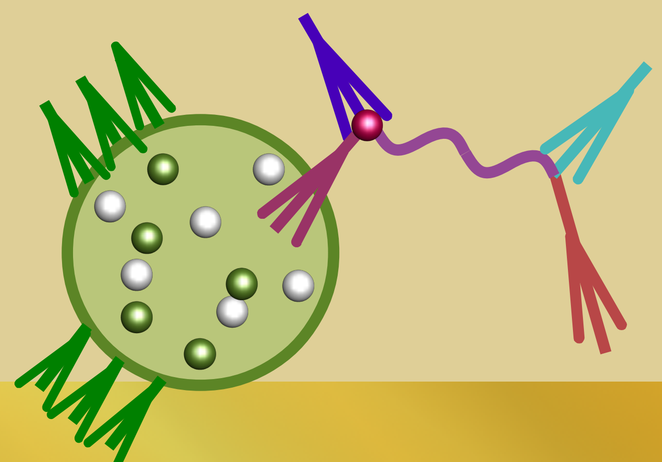

Final state interactions (FSI)

Their effect on the cross section is easy to understand in terms of the complex optical potential [(Horikawa et al., PRC **22**, 1680 (1980)]

$$E_{p'} = \sqrt{M^2 + p'^2} + U$$

- the real part modifies the struck nucleon's energy spectrum
- the imaginary part accounts for the attenuation of the single-nucleon final states

$$e^{i(E+U)t} = e^{i(E+U_V)t} e^{-U_W t}$$

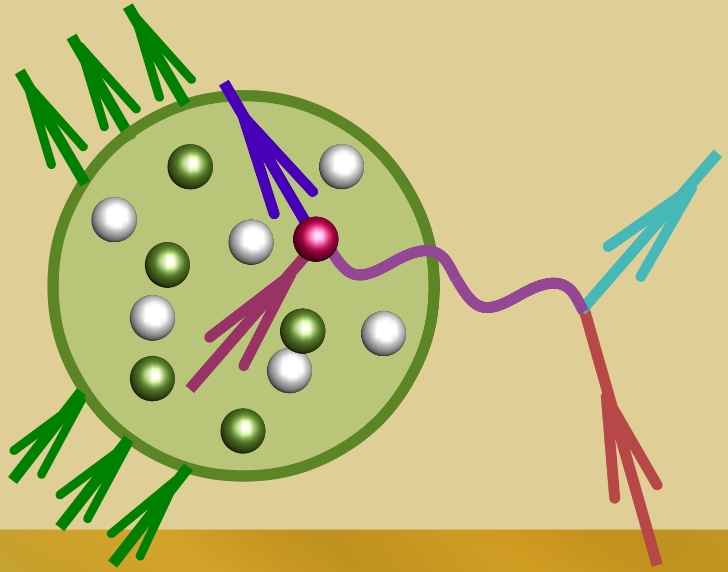

Final state interactions (FSI)

In the convolution approach,

$$\frac{d\sigma^{\mathrm{FSI}}}{d\omega d\Omega} = \int d\omega' f_{\mathbf{q}}(\omega - \omega') \frac{d\sigma^{\mathrm{IA}}}{d\omega' d\Omega},$$

with the folding function

$$f_{\mathbf{q}}(\omega) = \delta(\omega)\sqrt{T_A} + \left(1 - \sqrt{T_A}\right) F_{\mathbf{q}}(\omega),$$

Nucl. transparency

Nuclear transparency

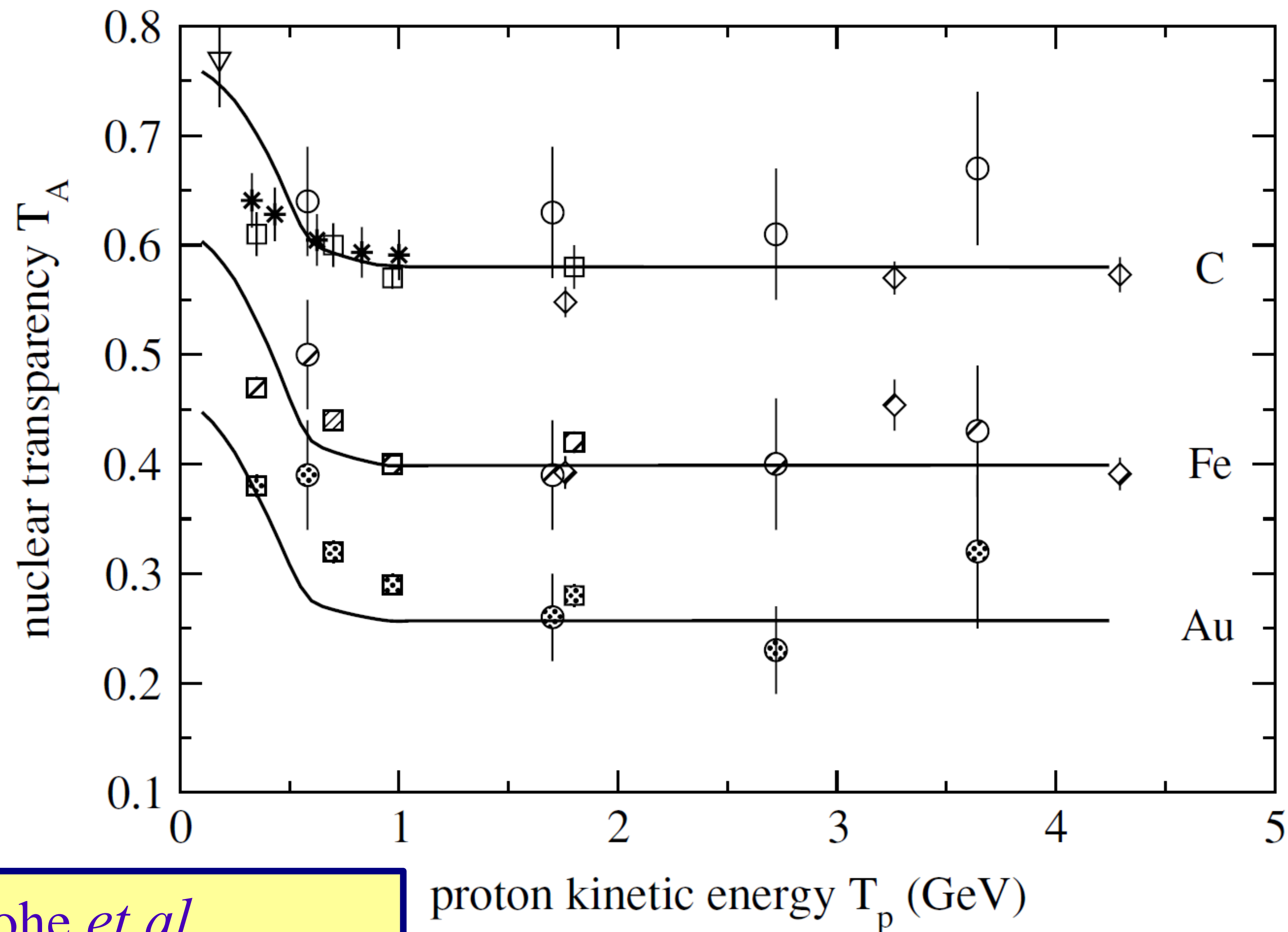

Rohe *et al.*,
PRC 72, 054602 (2005)

Real part of the optical potential

We account for the spectrum modification by

$$f_{\mathbf{q}}(\omega - \omega') \rightarrow f_{\mathbf{q}}(\omega - \omega' - U_V).$$

This procedure is similar to that from the Fermi gas model to introduce the binding energy in the argument of the δ function.

$$U_V = U_V(t_{\mathrm{kin}})$$

$$t_{\mathrm{kin}} = \frac{E_{\mathbf{k}}^2(1-\cos\theta)}{M + E_{\mathbf{k}}(1-\cos\theta)}$$

Real part of the optical potential

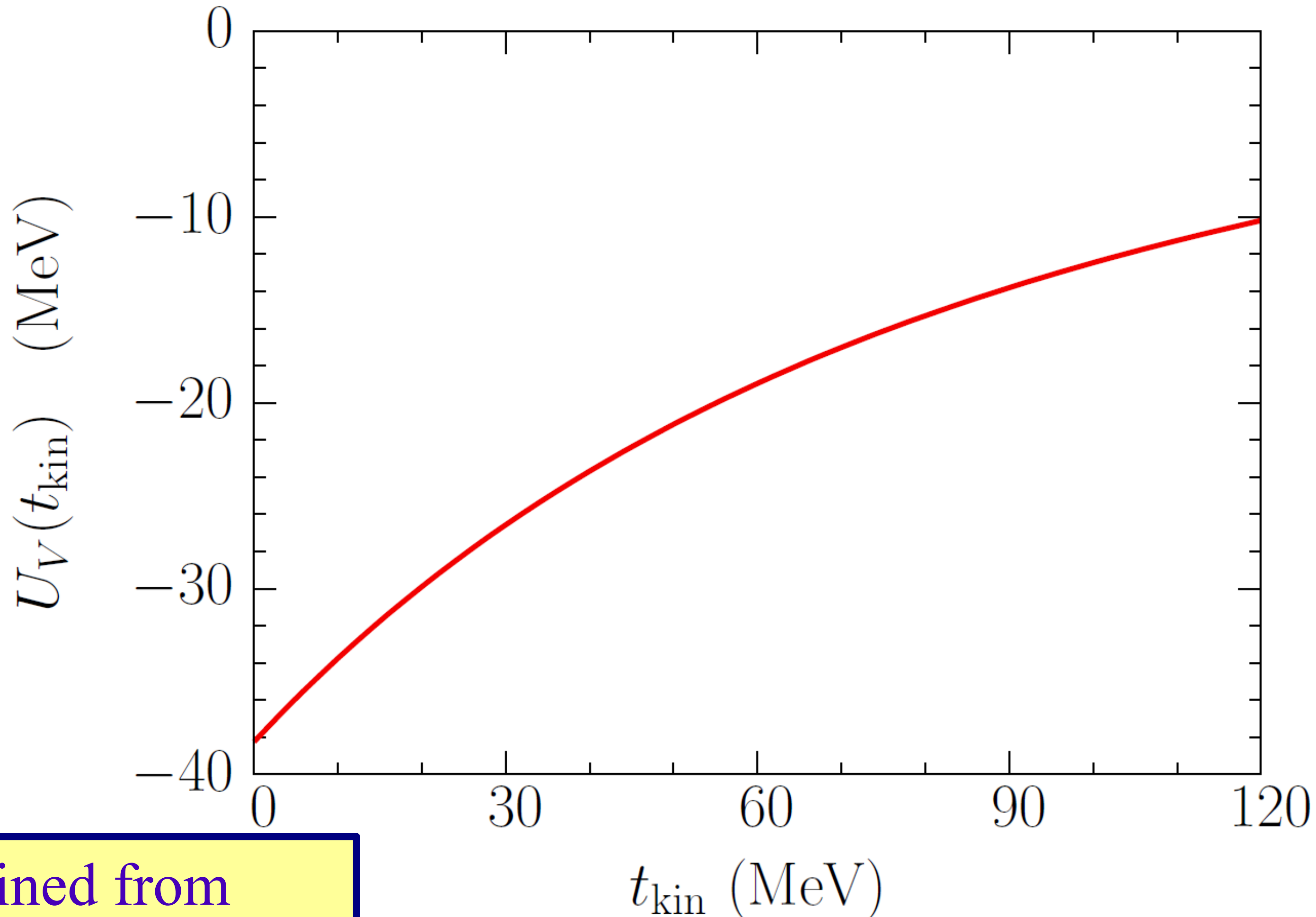

obtained from
Cooper *et al.*,
PRC 47, 297 (1993)

Optical potential by Cooper *et al.*

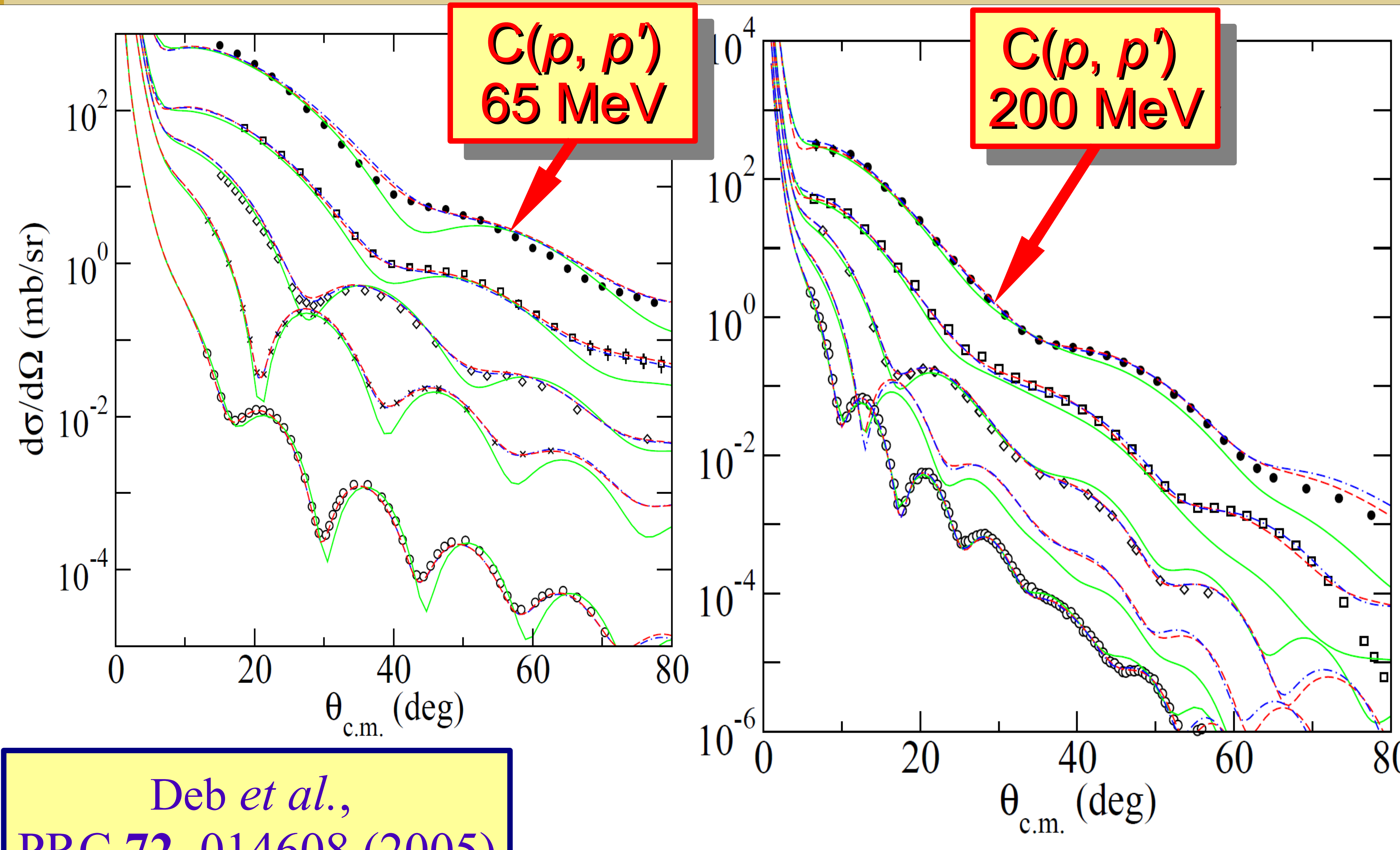

Deb *et al.*,
PRC **72**, 014608 (2005)

Comparisons to C(*e*, *e*′) data

Compared approaches

RFG model
$\varepsilon = 25$ MeV
$p_F = 221$ MeV

SF calculation without FSI

Our calculation, LDA treatment of Pauli blocking, Phys. Rev. D **82**, 013002 (2010)

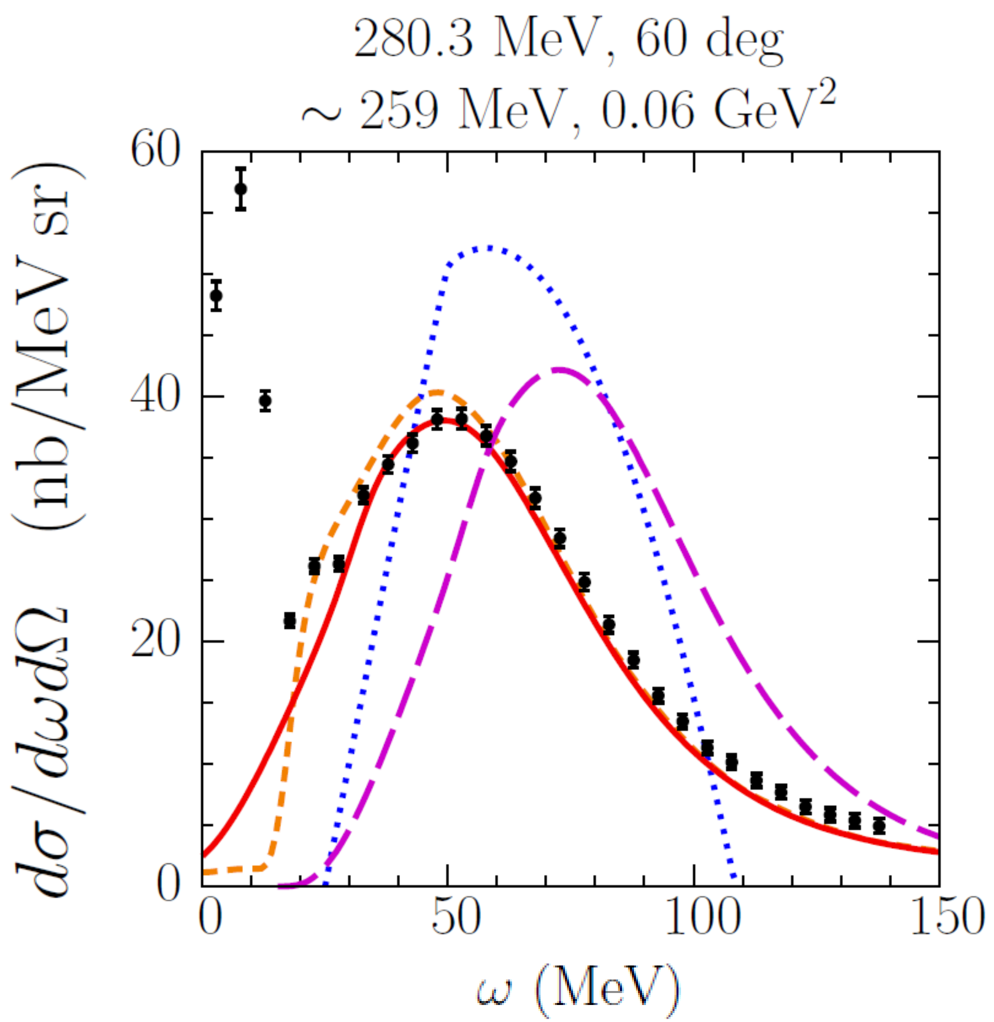

Our calculation, step function

Low excitation-energy phenomena

Calcs. include QE by 1-body current only

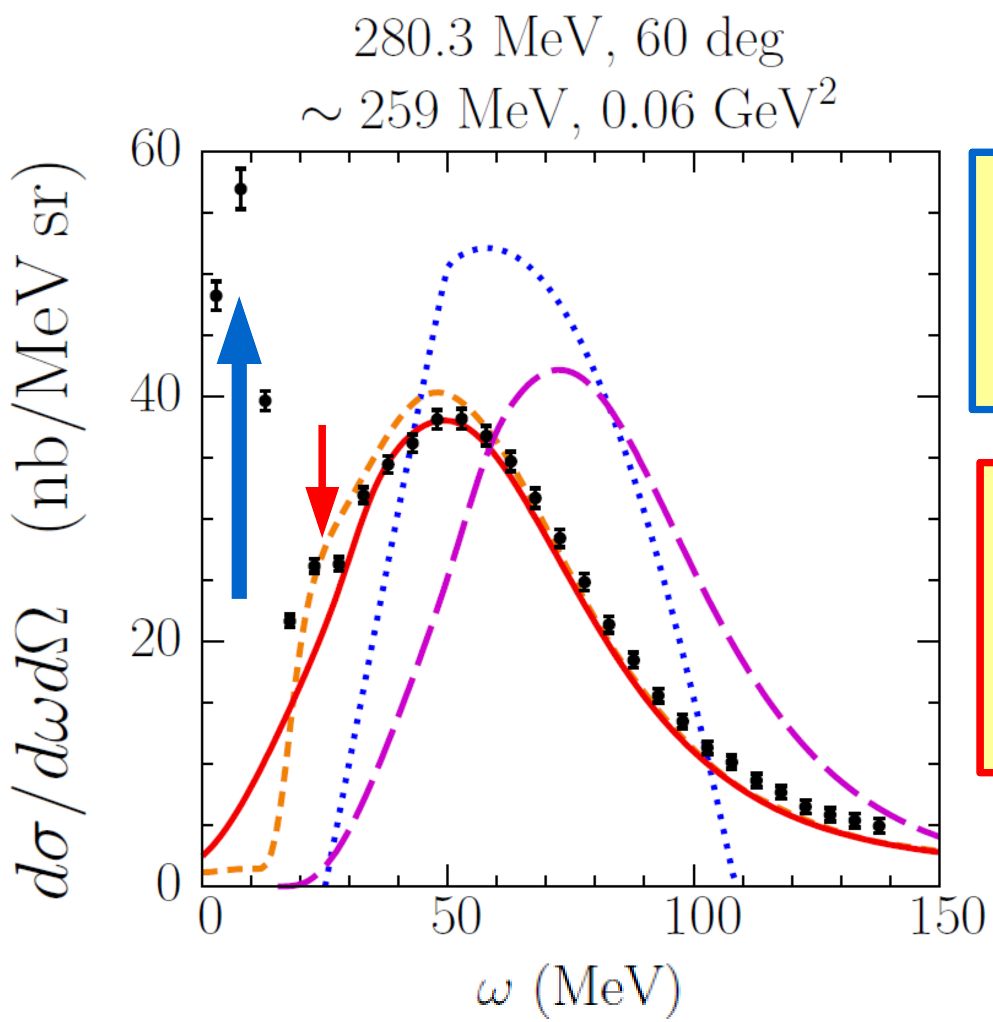

Elastic scattering and excitation of low-E_x levels

Giant resonance E_x = 22.6 MeV, Γ = 3.2 MeV

Comparisons to C(*e*,*e′*) data

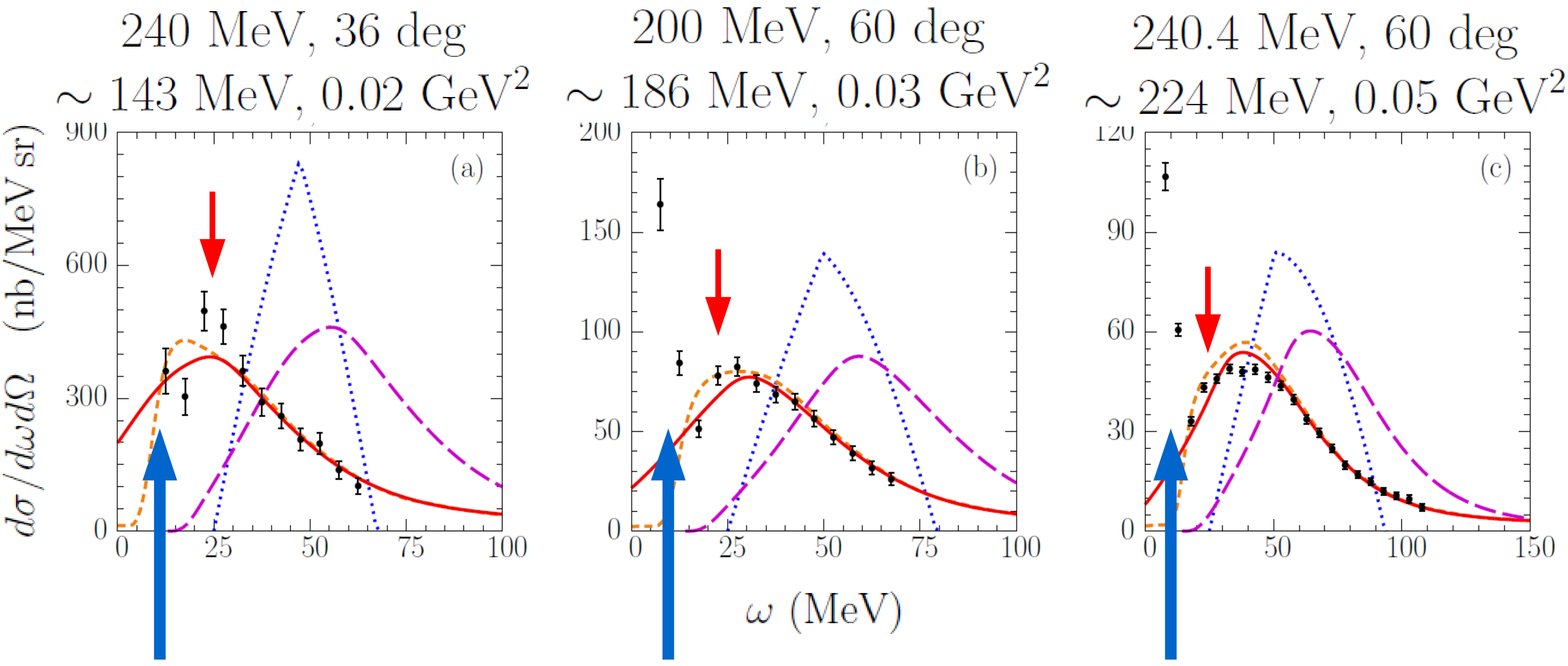

Barreau *et al.*,
NPA 402, 515 (1983)

Comparisons to C(*e*,*e*′) data

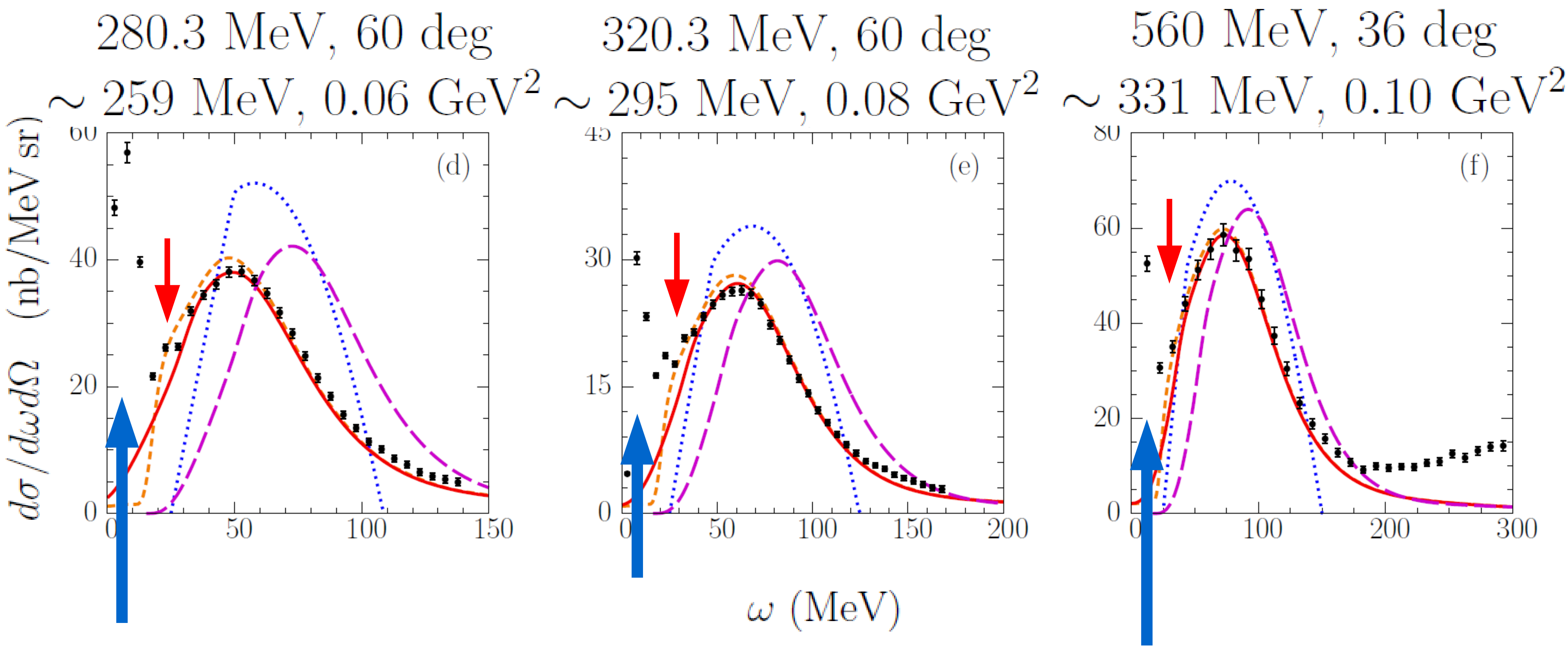

Barreau *et al.*,
NPA 402, 515 (1983)

Comparison to C(*e*,*e*′) data

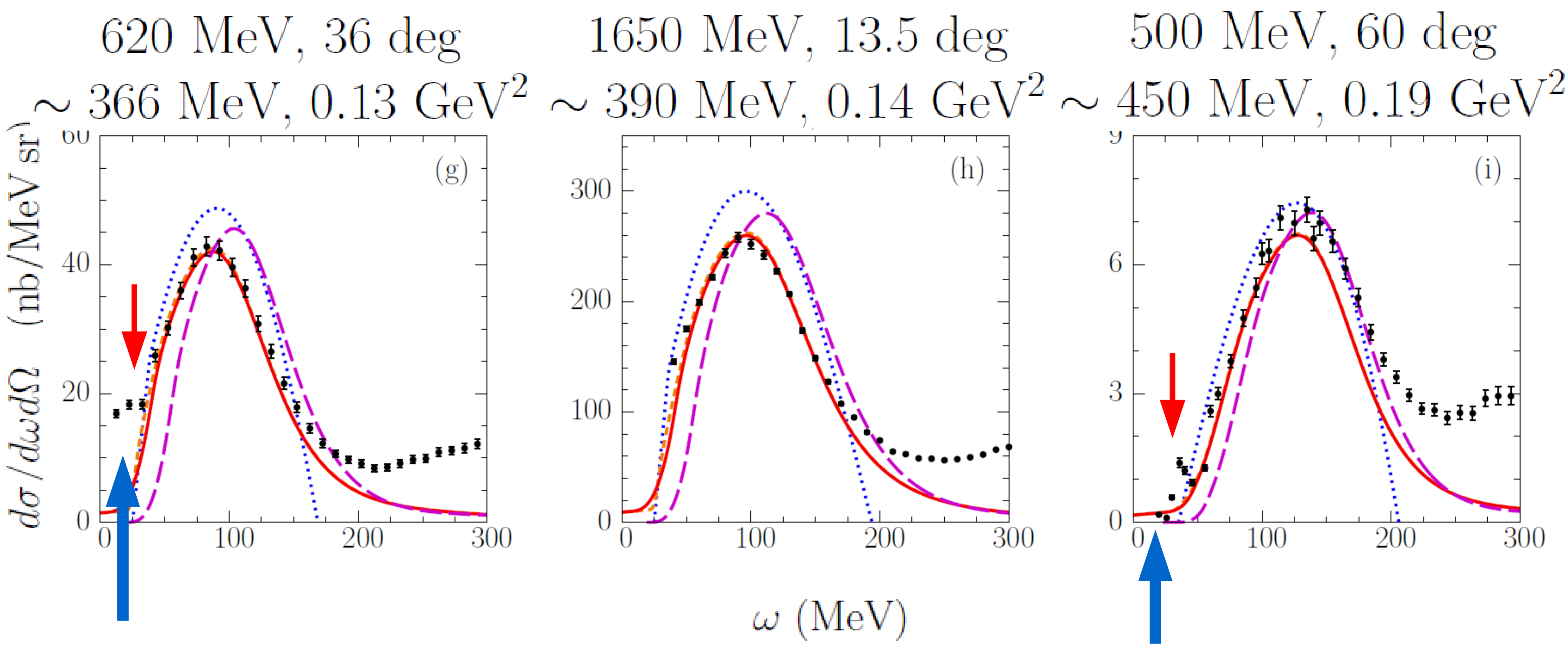

Barreau *et al.*,
NPA 402, 515 (1983)

Baran *et al.*,
PRL 61, 400 (1988)

Whitney *et al.*,
PRC 9, 2230 (1974)

Comparisons to C(e,e') data

In the supplemental material of **arXiv:1404.5687**
we show comparisons to the data sets collected
at **54 kinematical setups**

- energies from ~160 MeV to ~4 GeV,
- angles from 12 to 145 degrees,
- at the QE peak, values of momentum transfer from ~145 to ~1060 MeV/c and $0.02 \leq Q^2 \leq 0.86$ (GeV/c)^2 .

Comparisons to C(e,e') data

In the supplemental materia
we show comparisons to the
at **54 kinematical setups**

- energies from ~160 MeV to
- angles from 12 to 145 degre
- at the QE peak, values of m
  ~145 to ~1060 MeV/c and 0

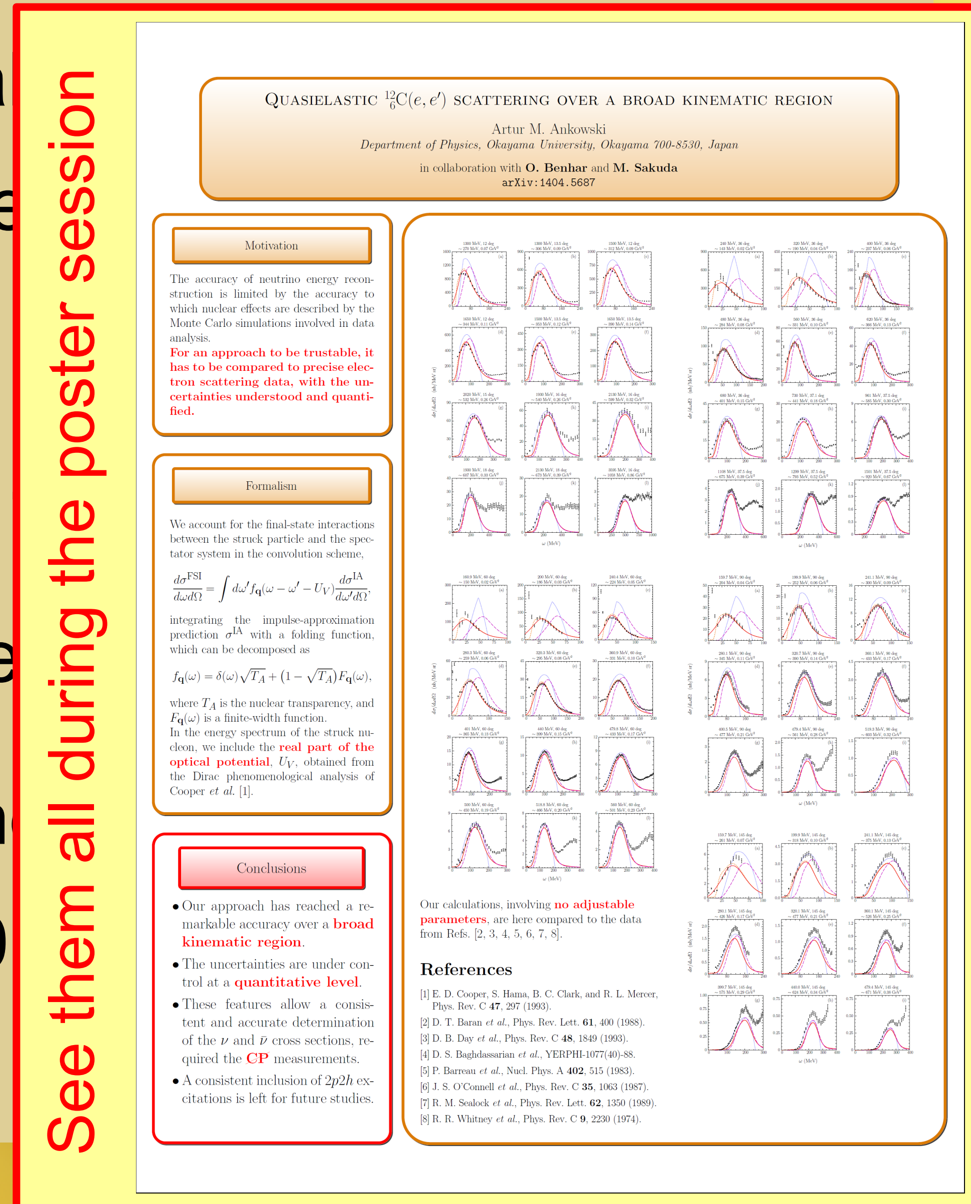

Neutrino energy reconstruction

Energy reconstruction

Consider the probability distribution that a muon of given energy and scattering angle is produced by a neutrino of energy E_ν

$$\mathcal{P}(E_\nu)\Big|_{E_\mu,\,\cos\theta} = \frac{\frac{d\sigma(E_\nu)}{dE_\mu\, d\cos\theta}}{\int dE_\nu \frac{d\sigma(E_\nu)}{dE_\mu\, d\cos\theta}}$$

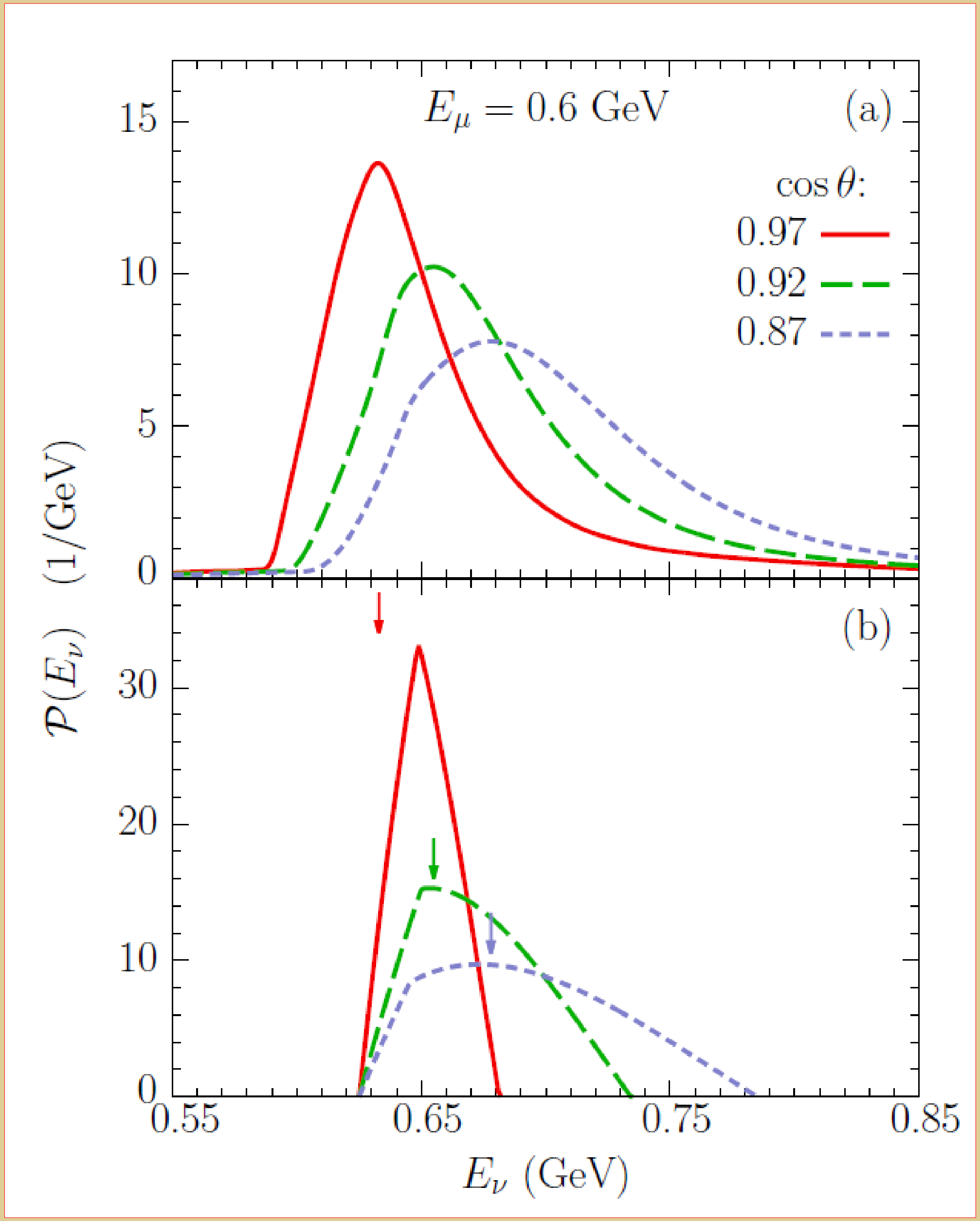

kinematics relevant to the T2K experiment

At cos = 0.97
the difference is ~16 MeV
for RFG with ε = 25 MeV

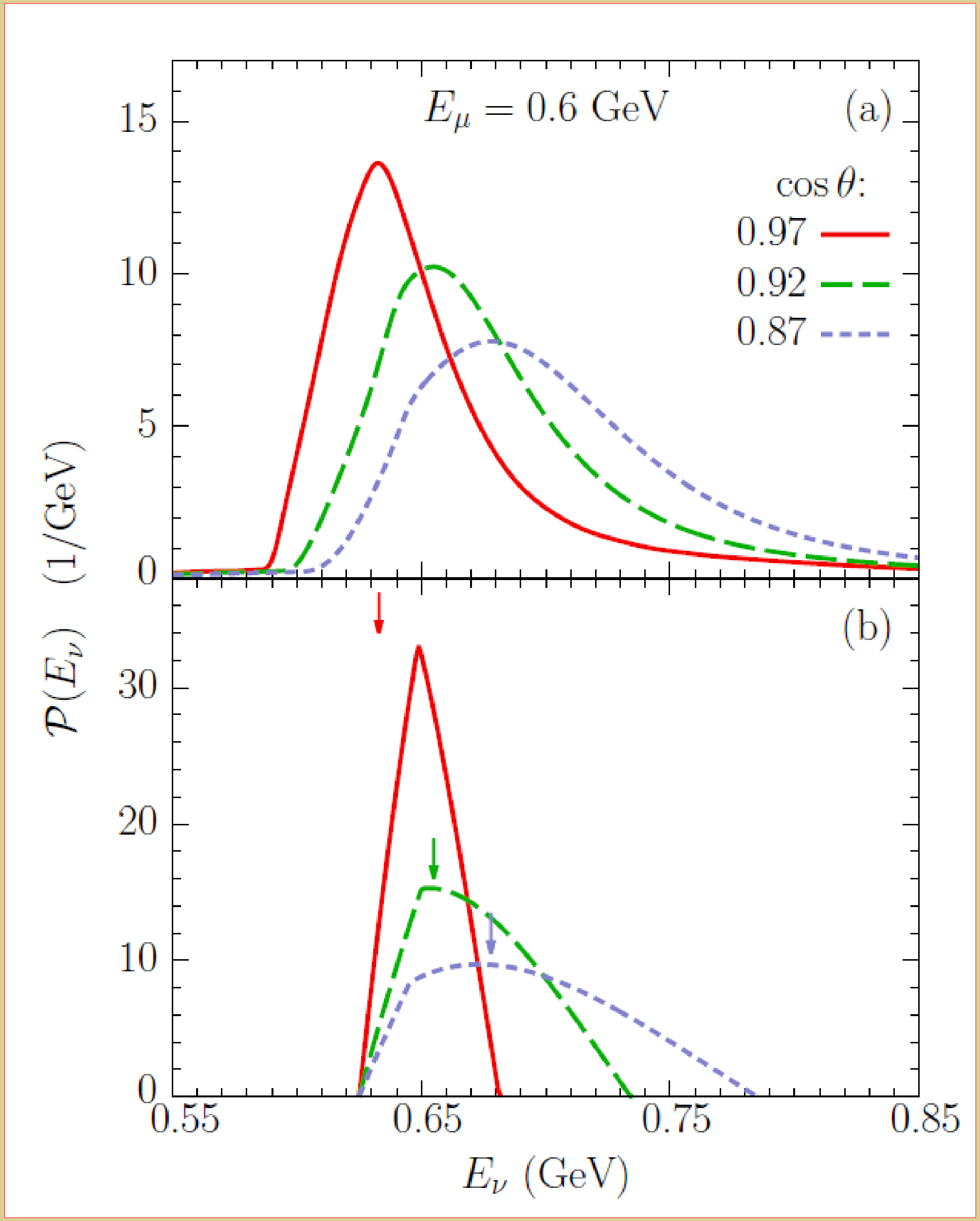

kinematics relevant to the T2K experiment

At cos = 0.97
the difference is ~16 MeV
for RFG with ε = 25 MeV

To get the maxima right

ε = 9 MeV @ cos = 0.97
ε =27 MeV @ cos = 0.92
ε =29 MeV @ cos = 0.87

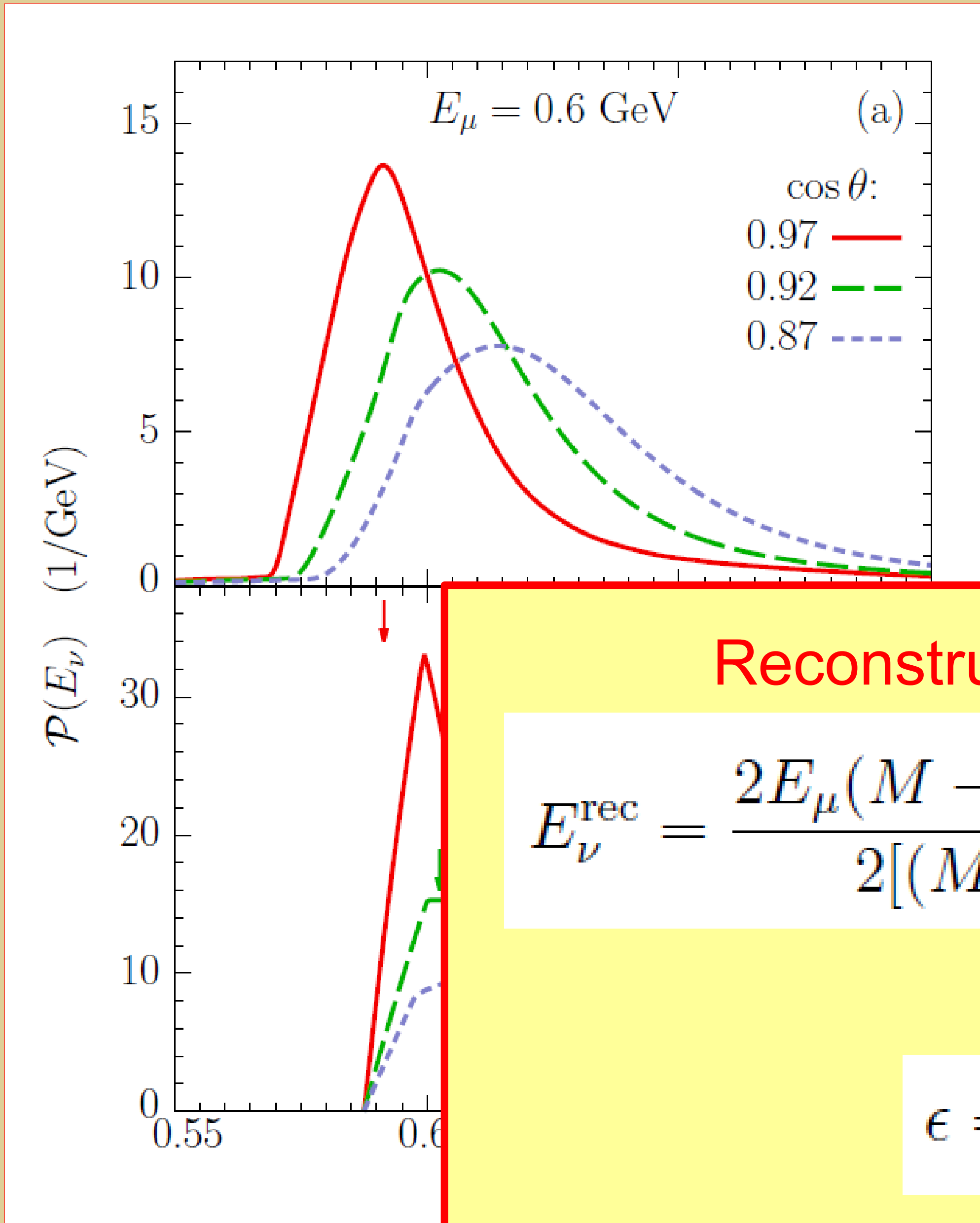

kinematics relevant to the T2K experiment

At cos = 0.97
the difference is ~16 MeV
for RFG with ε = 25 MeV

Reconstructing the energy from

$$E_\nu^{\text{rec}} = \frac{2E_\mu(M-\epsilon) - (M-\epsilon)^2 - m'^2 + M'^2}{2[(M-\epsilon) - E_\mu + |\mathbf{k}|_\mu \cos\theta)},$$

we need

$$\epsilon = \epsilon(\cos\theta, E_\mu)$$

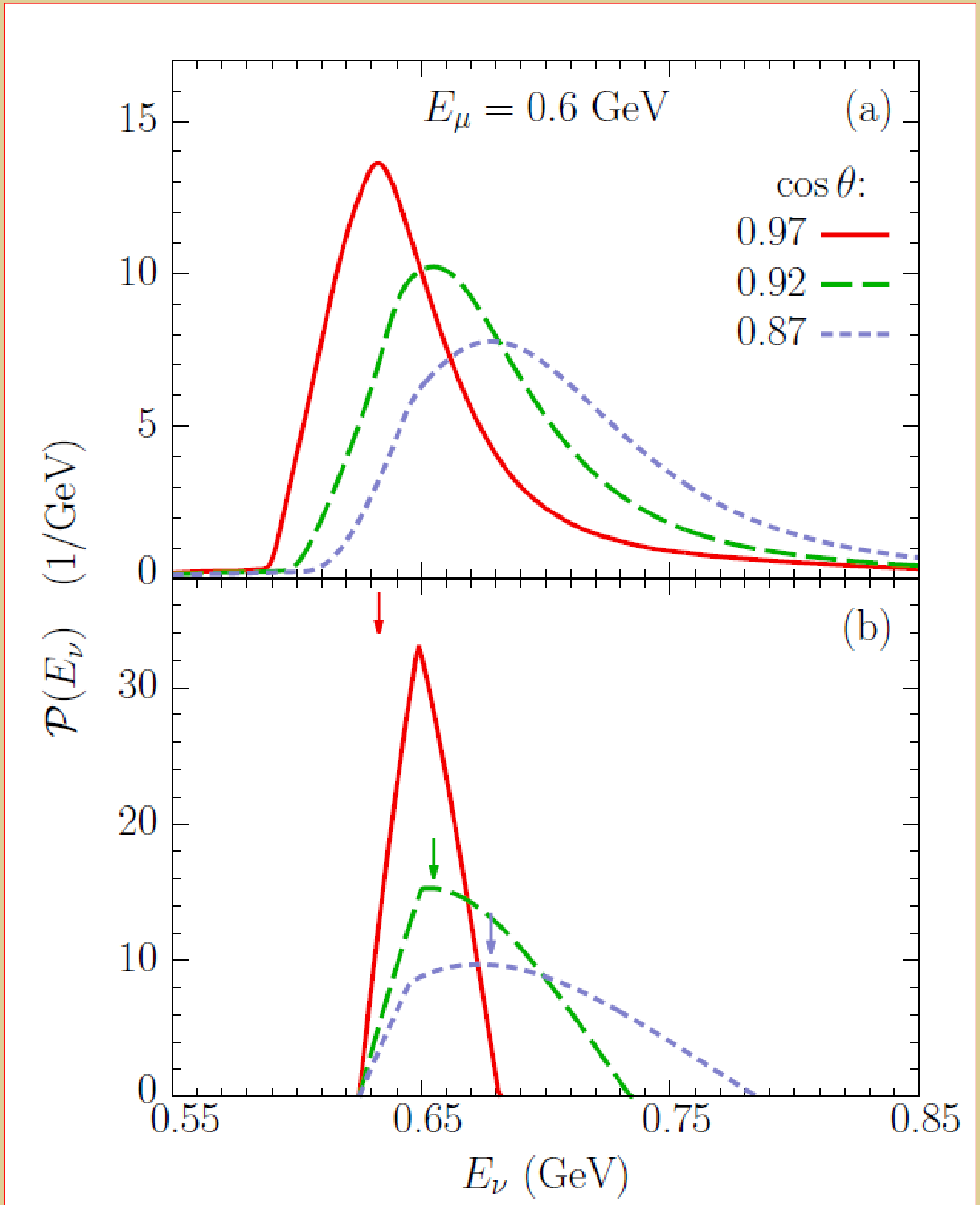
$E_\mu = 0.6$ GeV
(a)
cos θ:
0.97
0.92
0.87
(b)
$\mathcal{P}(E_\nu)$ (1/GeV)
E_ν (GeV)
0.55
0.65
0.75
0.85

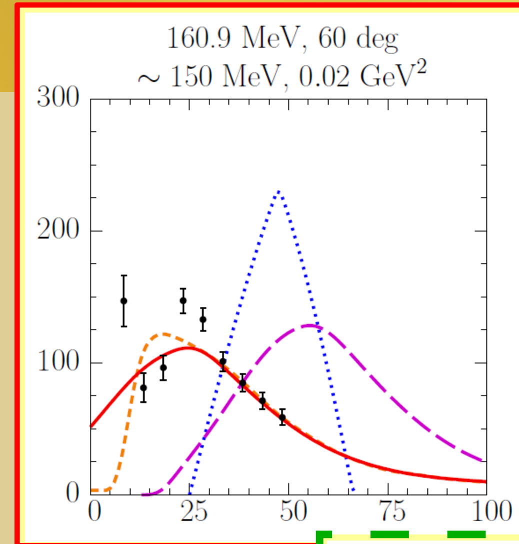
160.9 MeV, 60 deg
∼ 150 MeV, 0.02 GeV²

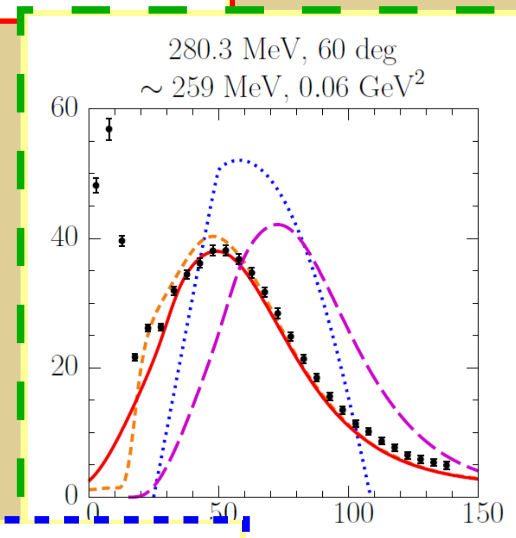
280.3 MeV, 60 deg
∼ 259 MeV, 0.06 GeV²

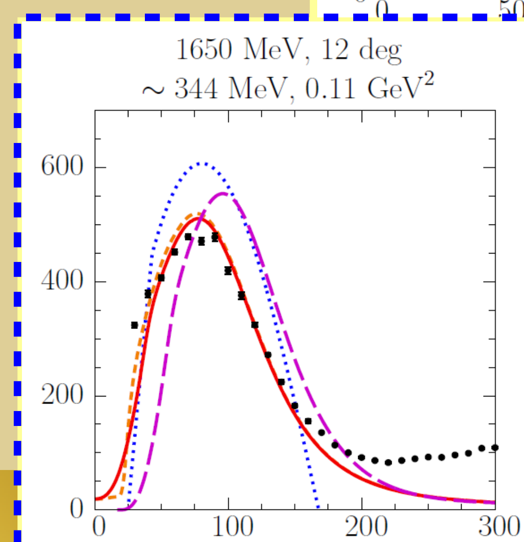
1650 MeV, 12 deg
∼ 344 MeV, 0.11 GeV²

Neutrino vs antineutrino

muon energy 600 MeV

	$\cos\theta = 0.97$	$\cos\theta = 0.92$	$\cos\theta = 0.87$
neutrino	633	655	678
antineutrino	619	639	661
difference	13.9	16.0	17.6

muon energy 400 MeV

	$\cos\theta = 0.97$	$\cos\theta = 0.92$	$\cos\theta = 0.87$
neutrino	422	435	444
antineutrino	406	421	428
difference	15.6	14.4	15.7

Summary

1. **The SF calculations accounting for FSI can describe the (*e,e′*) cross section down to |q|~150 MeV (Q^2~0.02GeV^2) accurately reproducing features of the QE peak.**

2. **An accurate description of nuclear effects is crucial for the accurate reconstruction of neutrino energy from the charged lepton's kinematics.**

3. **Accurate estimate of the neutrino-antineutrino difference is essential for determination of the CP violating phase.**

Backup slides

Nuclear transparency

O. Benhar @ NuInt05

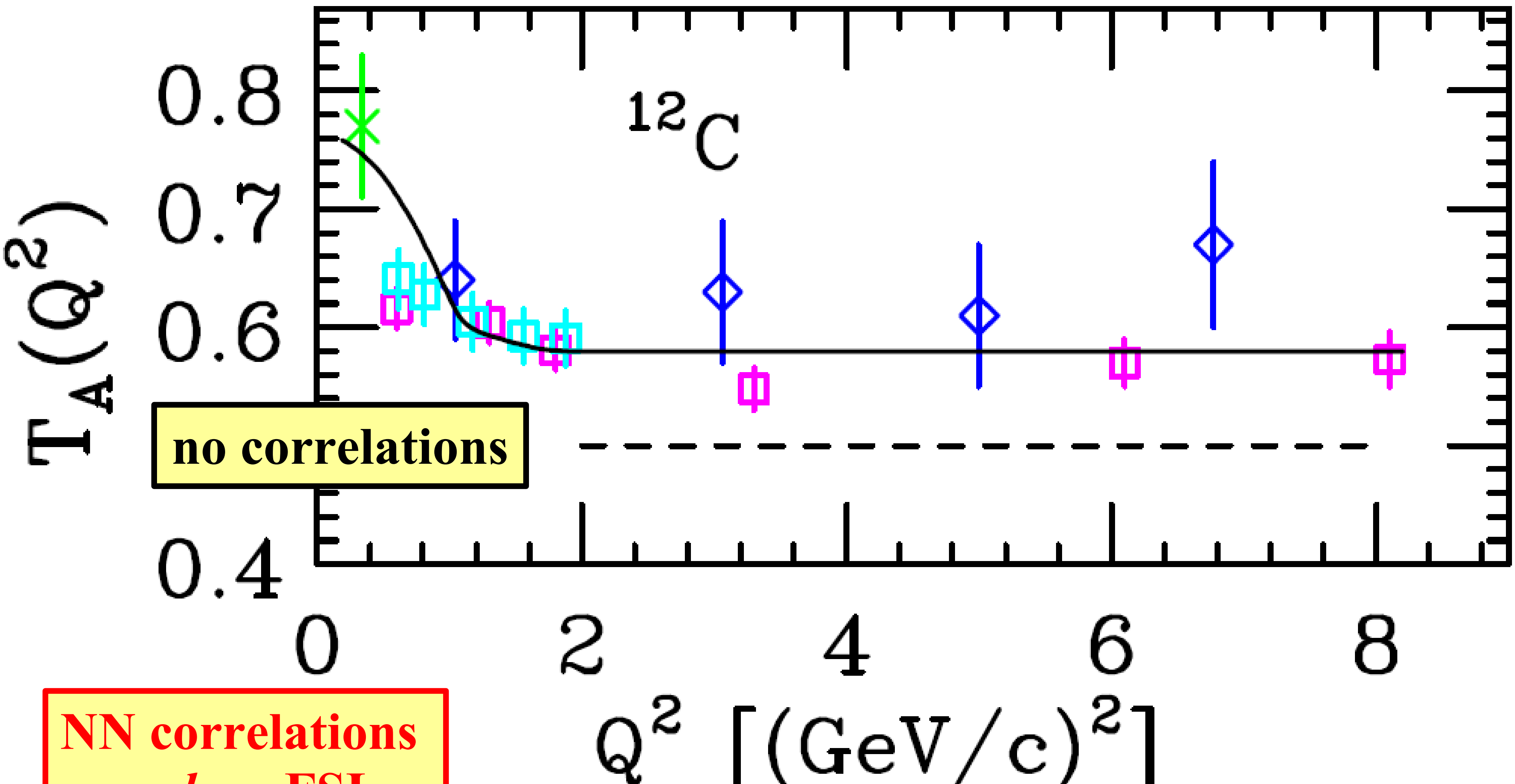

NN correlations *reduce* FSI

Quick and dirty comparison

Real part of the OP

- acts in the final state
- shifts the QE peak to low ω at low $|\mathbf{q}|$ (to high ω at high $|\mathbf{q}|$)

Binding energy

- acts in the initial state
- shifts the QE peak to high ω

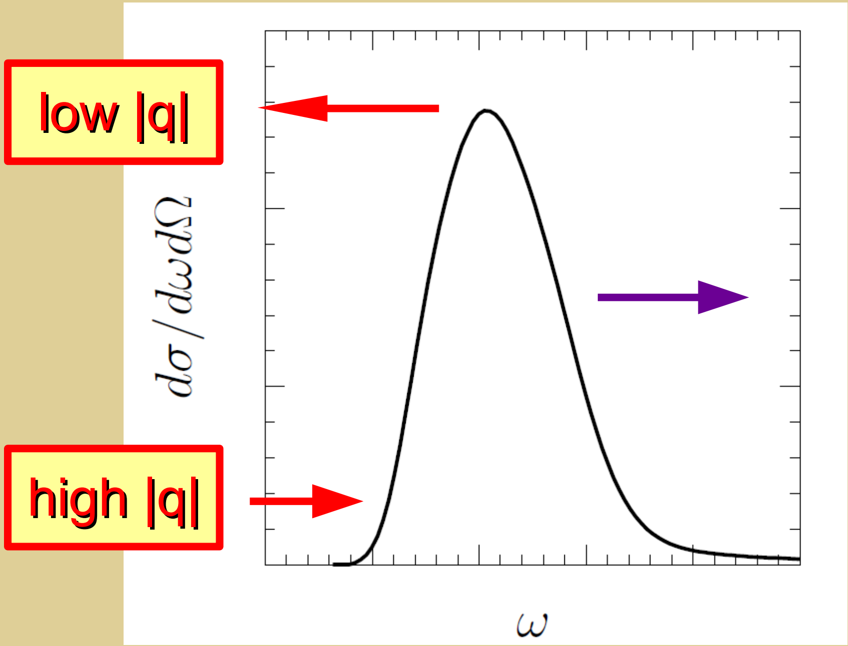

Neutrino vs antineutrino

muon energy 600 MeV

	cos θ = 0.97	cos θ = 0.92	cos θ = 0.87
neutrino	633	655	678
antineutrino	619	639	661
difference	13.9	16.0	17.6

muon energy 450 MeV

	cos θ = 0.97	cos θ = 0.92	cos θ = 0.87
neutrino	476	488	502
antineutrino	461	474	485
difference	15.1	14.5	16.9

Neutrino vs antineutrino

muon energy 700 MeV

	$\cos\theta = 0.97$	$\cos\theta = 0.92$	$\cos\theta = 0.87$
neutrino	736	768	801
antineutrino	723	752	782
difference	13.9	15.9	19.2

muon energy 500 MeV

	$\cos\theta = 0.97$	$\cos\theta = 0.92$	$\cos\theta = 0.87$
neutrino	529	542	561
antineutrino	515	528	544
difference	14.2	14.9	16.8

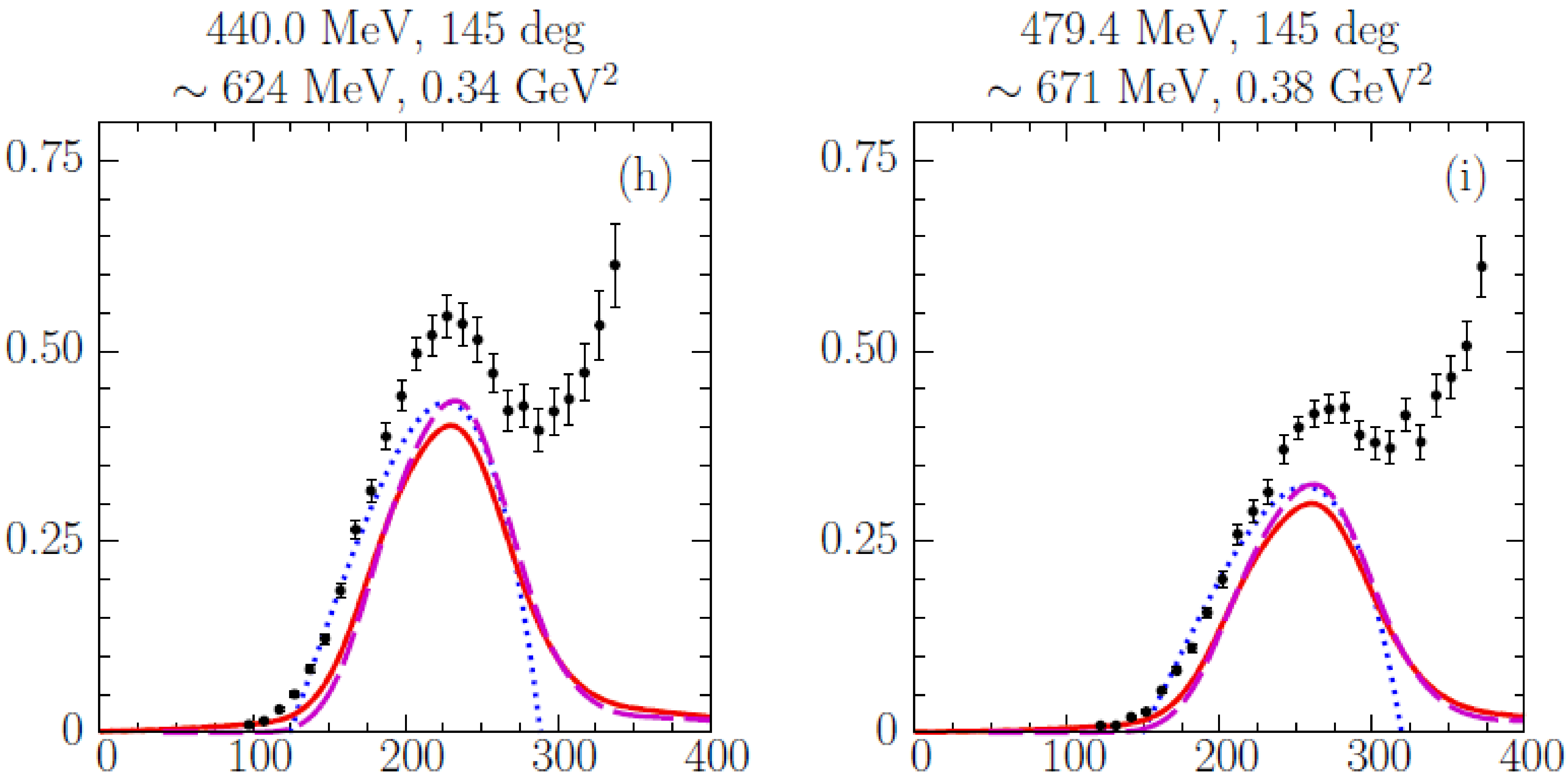
440.0 MeV, 145 deg
~ 624 MeV, 0.34 GeV^2
479.4 MeV, 145 deg
~ 671 MeV, 0.38 GeV^2
(h)
(i)
0
0.25
0.50
0.75
0
100
200
300
400